

Supplementary Information

Self-assembly of highly crystalline two-dimensional MOF sheets on liquid surfaces

Rie Makiura,^{*a,b} Kohei Tsuchiyama,^a Osami Sakata^{b,c}

^a Nanoscience and Nanotechnology Research Center, Osaka Prefecture University, Osaka 599-8531, Japan.

^b CREST, Japan Science and Technology Agency, Tokyo 102-0075, Japan

^c Japan Synchrotron Radiation Research Institute, Kouto 1-1-1, Sayo-cho, Sayo-gun, Hyogo 679-5198, Japan

*e-mail: r-makiura@21c.osakafu-u.ac.jp

Materials

5,10,15,20-tetrakis-(4-carboxyphenyl)-porphyrin-Co-(II) (CoTCPP) was purchased from Porphyrin Systems. Cu(NO₃)₂·3H₂O (>99.9%) and pure grades of pyridine, chloroform, and methanol were purchased from Waco Pure Chemical Industries Ltd or Junsei Chemical Co. Ltd. All chemicals were used as received without further treatment.

Substrate preparation

Silicon single crystals ((100) surface plane) were used as substrates in XRD and IR measurements. Amorphous quartz was used as a substrate for UV-vis absorption spectroscopic measurements. The Si(100) crystals were cut into 11 mm × 11 mm × 2 mm (thickness) sizes. The miscut angle of the (100) plane was less than 0.1°. The surface was polished to obtain a macroflatness of <0.01° and a microroughness (RMS) of <5 Å. Before the film fabrication, the substrates were immersed successively into ultrasonic baths of chloroform, acetone, and ethanol, each for 30 minutes.

Film preparation

0.2 mM or 0.04 mM of CoTCPP solution containing pyridine was prepared with a chloroform/methanol solvent (3:1, v/v). A PTFE Langmuir trough (375×75×5 mm, 0.16 L) was filled with 1 mM Cu(NO₃)₂·3H₂O aqueous solution as a subphase. The surface of the subphase was carefully cleaned by mild surface-touch vacuuming. CoTCPP/pyridine solution was spread onto the Cu(NO₃)₂ subphase with a microsyringe. Surface pressure–area (π -*a*) isotherm measurements were performed with a KSV minitrough system using a continuous pressing speed for two barriers of 10 mm/min. Waiting times until the motion of the barrier was initiated (WBG : waiting before go) were 1 and 60 minutes. The 2D array of CoTCPP-py-Cu at surface pressures of 0.5 and 5.0 mN m⁻¹ was deposited onto the substrate by the horizontal dipping method at room temperature - one side of the substrate surface approaches and makes contact with the subphase surface horizontally resulting in one layer deposition on one side of the substrate (process 1). The substrate with the CoTCPP-py-Cu sheet was then rinsed with flowing distilled water, immersed into distilled water for 3 minutes, and finally dried by blowing nitrogen (process 2). In order to stack additional layers, CoTCPP-py-Cu monolayers on the subphase were repeatedly transferred onto the substrate. The number of the layers deposited is controlled by the number of cycles of sheet deposition (process 1) and rinsing/solvent immersion/drying (process 2).

The same CoTCPP/pyridine solution was spread onto a pure water subphase for comparison. The two barriers were compressed at the same speed of 10 mm/min and the 2D array was again transferred onto the substrate at a surface pressure of 5.0 mN m⁻¹ by the horizontal dipping method.

UV-vis absorption spectra

UV-vis absorption spectra of the CoTCPP- py-Cu sheets on the quartz substrate were measured with a Jasco V-670

spectrophotometer at room temperature.

IR spectra

IR spectra were collected on a JASCO FT-IR 6200 spectrometer under vacuum condition at room temperature. A transmission method was applied for the film state samples fabricated on Si substrate.

Synchrotron XRD measurements

Synchrotron X-ray diffraction (XRD) data were collected at room temperature with a multiaxis diffractometer at beamline BL13XU ($\lambda = 1.555 \text{ \AA}$) in SPring-8. Helium gas was supplied through the cell during the measurement. Each dataset was recorded using a scintillation counter.

In the grazing incident X-ray diffraction (GIXRD) measurements, strong scattered intensity is observed when the X-ray incident angle (α) to the sample is below a critical angle. Optimized values of α were in the range $0.1\text{--}0.3^\circ$. A solar slit (0.4°) was placed between the sample and the detector to reduce background contribution.

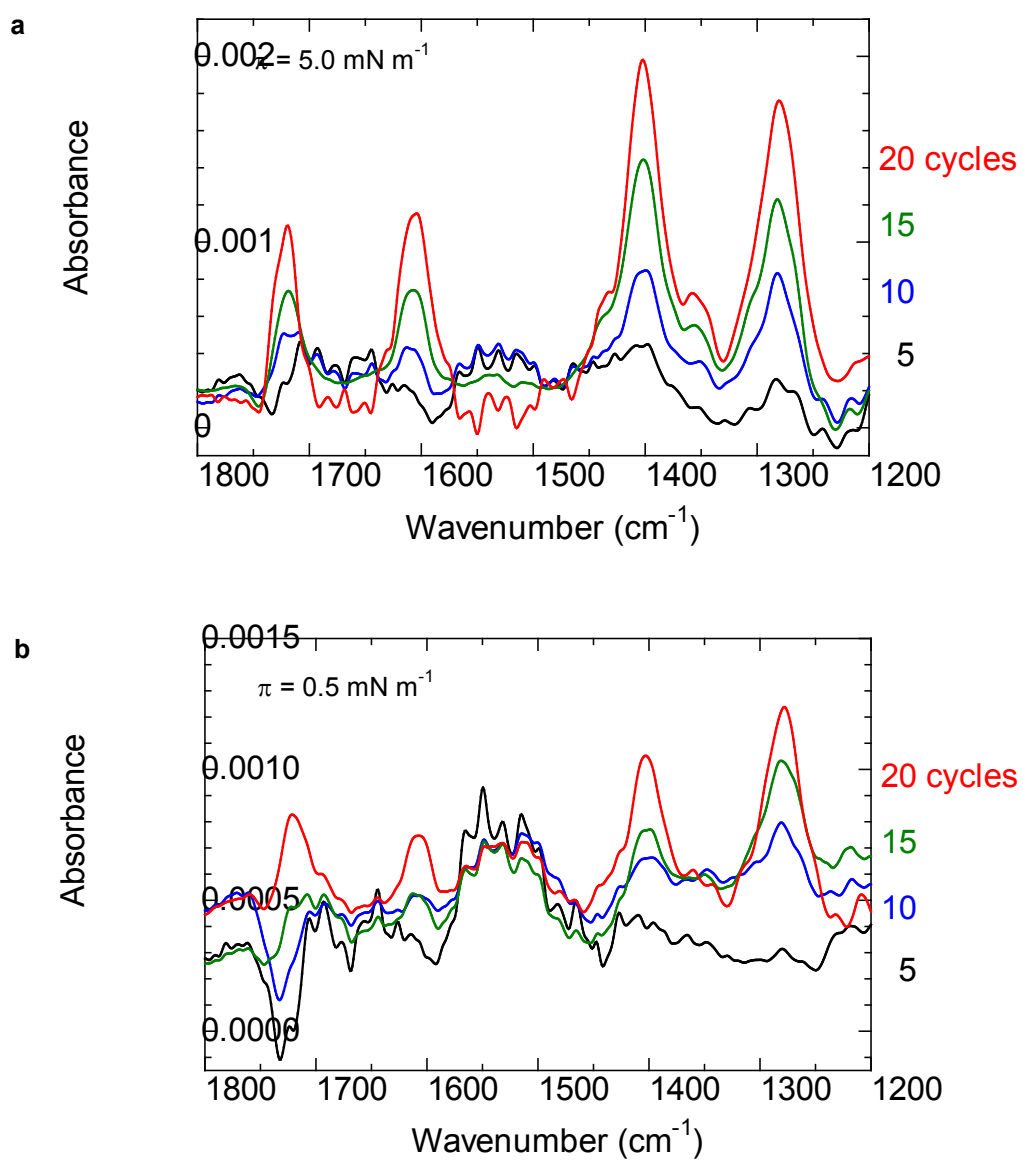


Figure S1 | IR spectra for NAFS-1. Evolution of IR spectra for the NAFS-1 films after successive deposition cycles at $\pi = 5.0 \text{ mN m}^{-1}$ **a**, and 0.5 mN m^{-1} **b**. The relatively weak absorbance observed for the film deposited at 0.5 mN m^{-1} compared to the film deposited at 5.0 mN m^{-1} is consistent with the UV-vis spectral measurement results (Fig. 2).

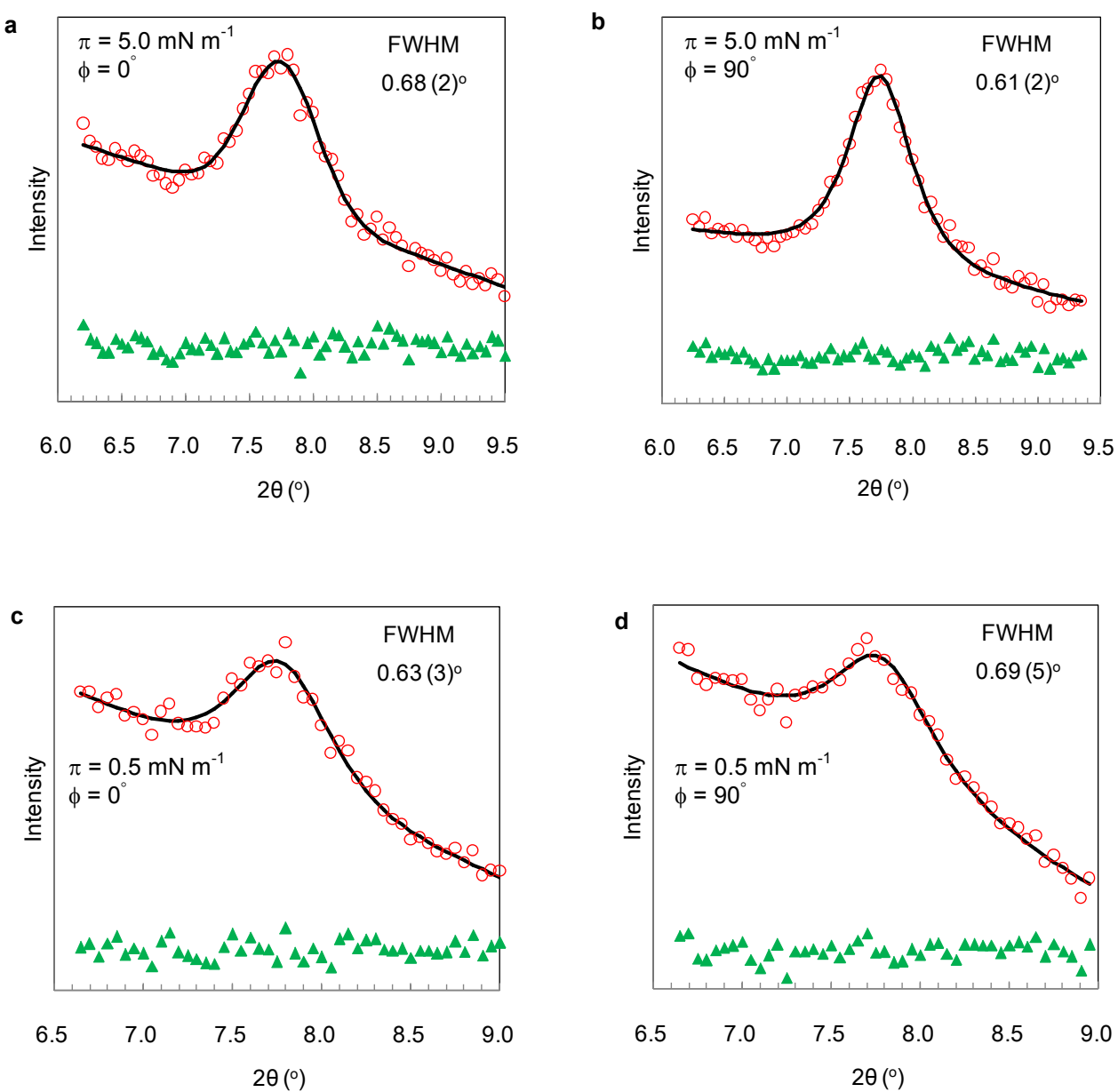


Figure S2| High-statistics in-plane GIXRD fine scans. Observed (red circles) and fitted (black solid line) in-plane synchrotron X-ray diffraction profiles (2θ scan, 2θ step = 0.05° , $\lambda = 1.555 \text{ \AA}$) in the vicinity of the (110) Bragg reflection for NAFS-1 thin films after successive deposition cycles at $\pi = 5.0$ **a,b**, and 0.5 mN m^{-1} **c,d** on Si(100) substrates. The lower green triangles show the difference profiles. The absence of azimuthal angle dependence in the diffraction profiles for both films indicates that the orientation of each sheet is random in the substrate surface and the pressing direction does not affect the sheet domain growth.

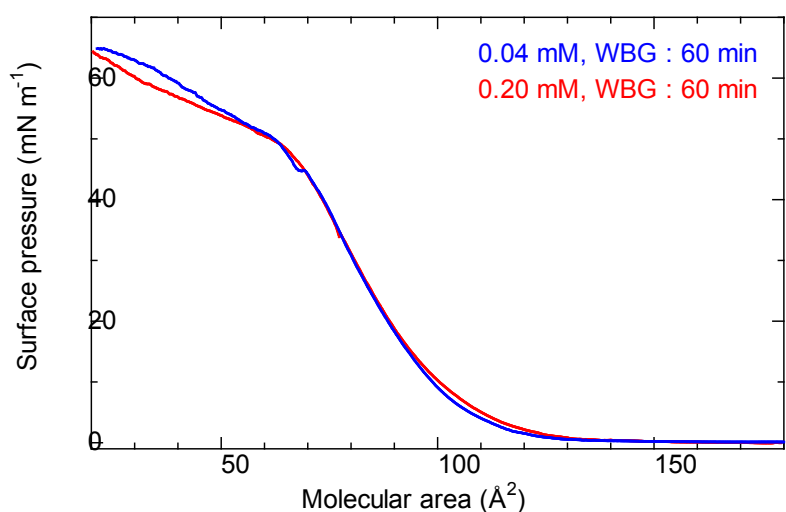


Figure S3| Surface pressure-area (π - a) isotherms for NAFS-1 arrays. The concentration of the spread solution (CoTCPP solution including pyridine) was 0.04 mM (blue solid line) and 0.20 mM (red solid line). The waiting time before compressing the surface by moving the barriers was 60 min for both solutions. The concentration of the spread solution did not affect the surface pressure evolution with changes in the molecular area.

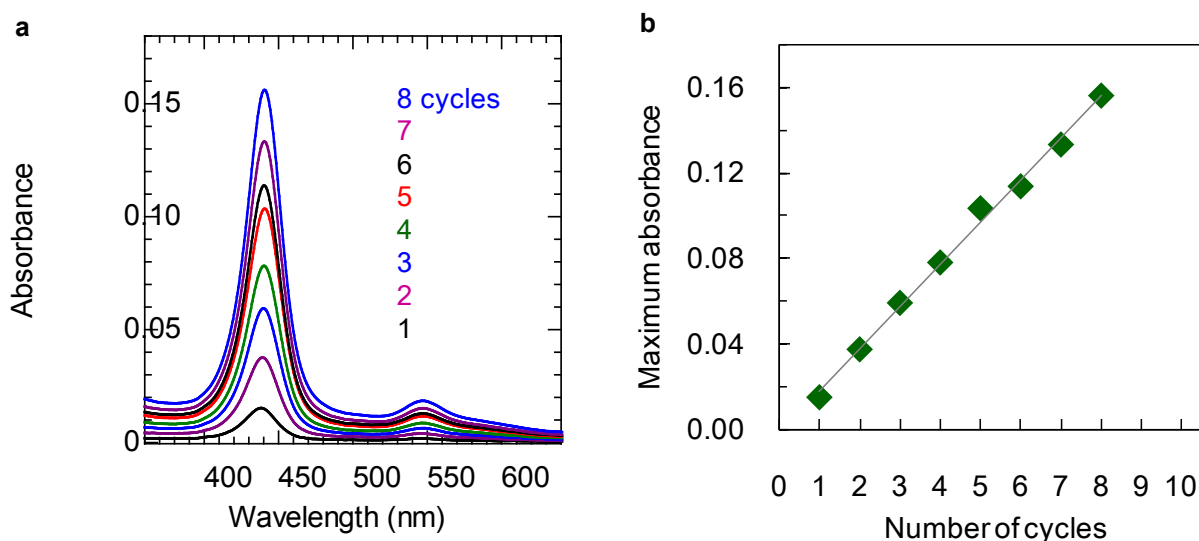


Figure S4| UV-vis spectra of the NAFS-1 nanofilm fabricated with 0.04 mM spread solution. (a) Evolution of UV-vis spectra for the film after successive cycles of sheet deposition at a surface pressure of 5.0 mN m^{-1} . **(b)** Plot of maximum absorbance of the CoTCPP Soret band versus the number of film growth cycles. A linear increase of the absorbance was observed with increasing number of cycles.

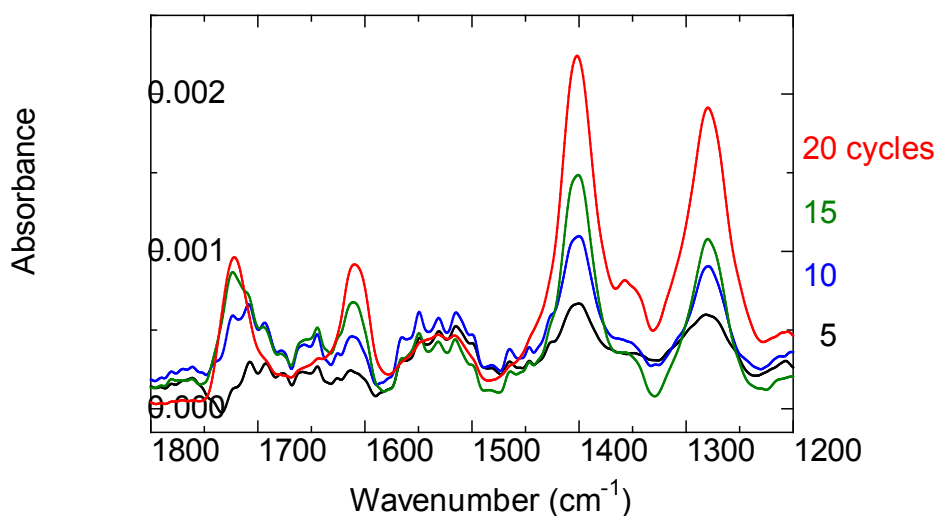


Figure S5| IR spectra for the NAFS-1 nanofilm fabricated with 0.04 mM spread solution. Evolution of IR spectra for the NAFS-1 films after successive deposition cycles.

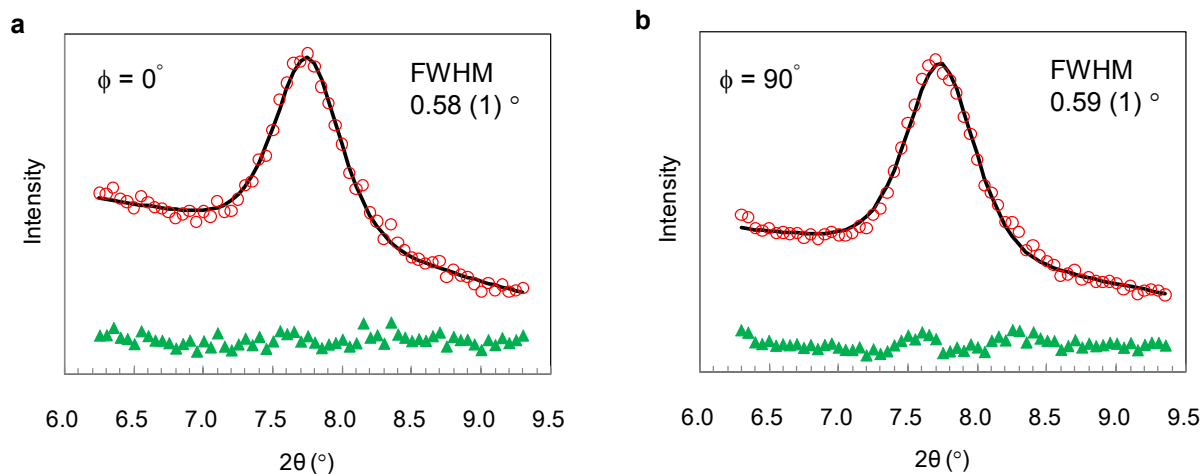


Figure S6 | High-statistics in-plane GIXRD fine scans of the NAFS-1 film fabricated with 0.04 mM spread solution. a,b, Observed (red circles) and fitted (black solid line) in-plane synchrotron X-ray diffraction profiles (20 scan, 2θ step = 0.05° , $\lambda = 1.555 \text{ \AA}$) in the vicinity of the (110) Bragg reflection for NAFS-1 thin films after successive deposition cycles at $\phi = 0^{\circ}$ **a** and 90° **b**. The lower green triangles show the difference profiles. The absence of azimuthal angle dependence in the diffraction profiles indicates that the orientation of each sheet is random in the substrate surface and the pressing direction does not affect the sheet domain growth.